future pharmacology

MDPI

Article

Production of Hydrogel-Based Curcumin-Loaded O/W Suspoemulsions

Timo Bodmer [1], Steffen F. Hartmann [2], Cornelia M. Keck [2], Martina Kleiner [1] and Karsten Köhler [1,*]

[1] Faculty of Life Sciences, Albstadt-Sigmaringen University, 72488 Sigmaringen, Germany
[2] Department of Pharmaceutics and Biopharmaceutics, Phillips-University Marburg, 35037 Marburg, Germany
* Correspondence: koehler@hs-albsig.de

Abstract: Curcumin is a biopharmaceutical classification system (BCS) class IV substance with many potential therapeutic effects. However, like many other BCS IV active pharmaceutical ingredients, complex formulations are needed to guarantee a sufficiently high bioavailability. A not-so-well-known delivery system is a suspoemulsion (SE). SEs are emulsions with a crystalline API in continuous or dispersed phases. This study aimed to produce curcumin-loaded o/w suspoemulsions with the particle in the oil phase for, e.g., encapsulation or triggered release effects. The particles need to be smaller than the emulsion droplet size to attain high encapsulation efficiencies (EE) in the oil phase. Sonofragmentation and bead milling were tested for their ability to produce these nanocrystals in different dispersion media. It was discovered that production in miglyol was the best fit for the needed application of the crystals in SEs. Around 85% (by volume) of the particles produced with bead milling were smaller than the droplet size of about 5 µm. In contrast, only 23% of the sonofragmentated particles were below the diameter of those droplets. This oily suspension was then used to successfully produce hydrogel-based o/w suspoemulsions. In the second part of this study, we investigated different methods for determining encapsulation efficiency, but none of the methods accurately and satisfactorily resolved the encapsulation efficiency. Finally, the suspoemulsions could not be macroscopically distinguished from one another and were physically stable. In summary, we showed that stable hydrogel-based curcumin-loaded o/w suspoemulsions could be produced.

Keywords: curcumin; suspoemulsion; bead milling; sonofragmentation; encapsulation; nanocrystals; submicron crystals; delivery system

Citation: Bodmer, T.; Hartmann, S.F.; Keck, C.M.; Kleiner, M.; Köhler, K. Production of Hydrogel-Based Curcumin-Loaded O/W Suspoemulsions. *Future Pharmacol.* **2023**, *3*, 451–463. https://doi.org/10.3390/futurepharmacol3020028

Academic Editors: Francesco Maione and Ali Zarrabi

Received: 10 February 2023
Revised: 5 April 2023
Accepted: 21 April 2023
Published: 27 April 2023

1. Introduction

Increasingly more active pharmaceutical ingredients (APIs) with low solubility in water and/or poor permeability have gained attention in recent years. In 2012, it was estimated that 70–90% of new small molecule drugs were in the biopharmaceutical classification system classified as a class II or class IV API [1,2]. Curcumin is one of these drugs, classified as a BCS class IV substance [2].

The term curcumin is used rather unspecifically in the literature. It is often used to refer to *Curcuma longa* L. extract. Occasionally, it refers to the pure substance [3]. However, herein, curcumin is used to denote the extract, typically containing up to 80% curcumin, at least 3% bisdemethoxycurcumin (BDC), and at least 15% demethoxycurcumin (DMC) [3]. Because of its vast number of various targets, curcumin could potentially be used in many different therapeutic fields, e.g., for its anti-inflammatory, antioxidative, tumor preventive, antibacterial, or antidepressant effects, among others [4–8]. Apart from those promising factors, we chose this yellow-orange substance as a model drug because of its beneficial optical properties [9].

There are many different approaches to the formulation of curcumin, with some leading to better bioavailability. Aside from existing lipid-based and polymer-based delivery systems, different emulsions, and molecular complexes [10–13], nanocrystals show

great promise, especially in cases in which (trans)dermal delivery is necessary [14–16]. Suspoemulsions (SEs) are another such new concept.

A suspoemulsion is the combination of an emulsion and a suspension. Suspoemulsions are primarily utilized in agriculture when two or more active ingredients (AIs) or an AI and adjuvants with different physical properties are used in one formulation [17]. Therefore, it can be assumed that SEs can lead to increased uptake of AI into plants [18,19]. Depending on the location of the suspension (continuous phase or the dispersed phase), two SE types can be distinguished [19]. While particles in the continuous phase (Figure 1III) are attractive for (most) applications in agrochemistry, the encapsulation of particles in the dispersed phase (Figure 1IV) has vast potential for application in pharmatechnology. Suspoemulsions, as delivery systems, were first described by Schmidt and Perschbacher et al. [20] in 1989 for parenteral use in animals. However, to our best knowledge, SEs were not yet described as (trans)dermal delivery systems. Aside from the description of using an SE for producing polymeric microspheres [21], there have been no publications addressing SEs, in a pharmaceutical context, since the 1990s.

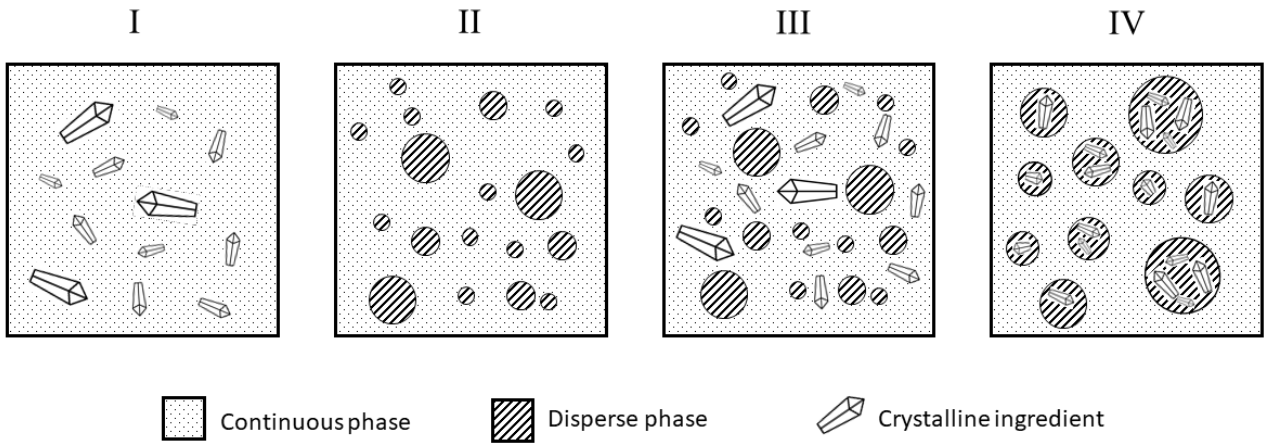

Figure 1. Schematic illustration of (**I**) a suspension, (**II**) an emulsion, (**III**) a suspoemulsion with the crystalline ingredient in the continuous phase, and (**IV**) a suspoemulsion with the crystalline ingredient encapsulated in the dispersed phase.

There are many advantages offered by SEs. The high local concentration of crystalline API results in a high concentration gradient with a depot effect. Additionally, the sedimentation effects of larger particles, decreasing the amount and the depth of penetration, as occurs in the dermal application of nanosuspensions, could be prevented [14]. Furthermore, it is well known that various oils can act as penetration enhancers [22–24]. A closer association of the API with this adjuvant—as is the case in o/w suspoemulsions—could further enhance this effect. This effect was already shown in the cuticles of plant leaves [18]. However, as indicated earlier, related studies on vertebrates are scarce.

Nonetheless, for the further study of SEs' potential pharmaceutical applications, high amounts of the API, encapsulated during formulation, are desirable. Therefore, this study aimed to produce a physically stable hydrogel-based o/w curcumin suspoemulsion with curcumin encapsulated in the oil phase. In this study, curcumin was used as a model API to demonstrate the fundamental formulation principle. We chose a gel for the continuous water phase to stabilize the suspoemulsion via a yield point. With this approach, we were able to reduce the number of emulsifiers, as well as their amount, thus presumably leading to a simpler and more stable system.

In the first step, an oil-based nanosuspension was produced. Different techniques have been shown to be able to produce nanoparticles in the needed size range. These include, for example, a kneading technique, stirred media milling/small-scale bead milling, disc mills, high-pressure homogenizers, roller mills, or ultrasonic homogenizers [25]. This paper reports on sonofragmentation (ultrasonic) and bead milling in aqueous and oily

media. These two processes were chosen because they are known to produce the smallest particles, primarily due to their high energy inputs into the system and their high stress intensities [25]. Two different processes could be suitable to obtain a curcumin suspension in oil. In the first (I), the curcumin is dispersed in water and ground to obtain the required particle size. The particles are then dried and redispersed into the oil phase. However, there is a risk that new agglomerates will form during the drying process, and transferring the curcumin into the lipophilic phase can prove challenging. The second (II) and more straightforward process involves the dispersal of the curcumin in oil, followed by grinding. In this paper, we compared both methods.

In a second step, suspoemulsions with different particle sizes were produced, and different methods to determine encapsulation efficiency, such as photometric measurement, were investigated.

2. Materials and Methods

2.1. Materials

Curcumin was purchased as a 95% extract from Azafran GmbH (Klein Offenseth-Sparrieshoop, Germany). Lysolecithin (1-Palmitoylphosphatidylcholine) from Dragonspice Naturwaren (Reutlingen, Germany) and TPGS (D-α-Tocopheryl-polyethylene-glycol-1000-succinate; HLB-value 13.2) from Caesar and Loretz GmbH (Hilden, Germany) were used as steric stabilizers of the curcumin particles and as o/w-emulsifier. The medium-chain glycerides (miglyol 812), glycerol (85%), and hydroxyethylcellulose 10,000 mPs (HEC) were obtained from Caesar and Loretz GmbH (Hilden, Germany). To measure the standard curve, polysorbate-20 (Tween® 20) from Caesar and Loretz GmbH (Hilden, Germany) was used. Rapeseed oil, used for laser diffraction analysis, was purchased at a local grocery store.

2.2. Methods

2.2.1. Particle Size Analysis

The particle size distributions of the curcumin suspensions were measured with laser diffraction analysis, carried out with a Mastersizer 2000 (Malvern Instruments, Malvern, UK). The measurement data were analyzed using the Mie Theory. The real refraction index for curcumin was set, for all wavelengths, at 1.87. The imaginary refractive index was set at 0.1 for 466 nm (blue light source) and 0.01 for 633 nm (HeNe-Laser). Initial attempts to measure the particle sizes directly in miglyol failed due to its high viscosity, which led to many entrapped air bubbles that could not be removed before the sample material was added. While we were aware that the results could be slightly impacted, a dilution in rapeseed oil (refractive index 1.4706), with lower viscosity, was conducted. The sample of the nanocrystalline curcumin was taken directly after the milling process. A suspension of the bulk curcumin was produced in miglyol before measurements were taken, containing the same concentrations (*w/w*) of curcumin and lysolecithin (respectively, in water with TPGS) as in the bead-milling process. Using a previously performed method of development, the settings of the diffractor's sampling chamber (700 rpm for the stirrer and 30% ultrasonic intensity) were found to be optimal. As such, 30 s after the sample was added to the sampling chamber, measurement began. The introduction of bubbles into the system during the addition of the samples was found to be critical.

Some light microscopic pictures were taken as control using a Nikon Eclipse E600W (Nikon Corporation, Tokyo, Japan).

The emulsion droplet size (emulsion was produced without the curcumin) was also measured using laser diffraction analysis. The refractive index for miglyol was set to 1.4493. The refractive index of the dispersant (water) was set to 1.33.

2.2.2. Production of Curcumin Suspension

In this paper, we investigated two possible processes (see Figure 2). The first process involved the production of a water-based curcumin suspension. Subsequently, these

submicron particles had to be transferred into the oil phase. To transfer the particle between the phases, an additional drying step (e.g., using a drying oven or freeze-drying), followed by a redispersion, was considered as a potentially suitable process. For the water-based curcumin suspension, we used the bead-milling process, as successfully established by Pelikh and Keck (2020) [15].

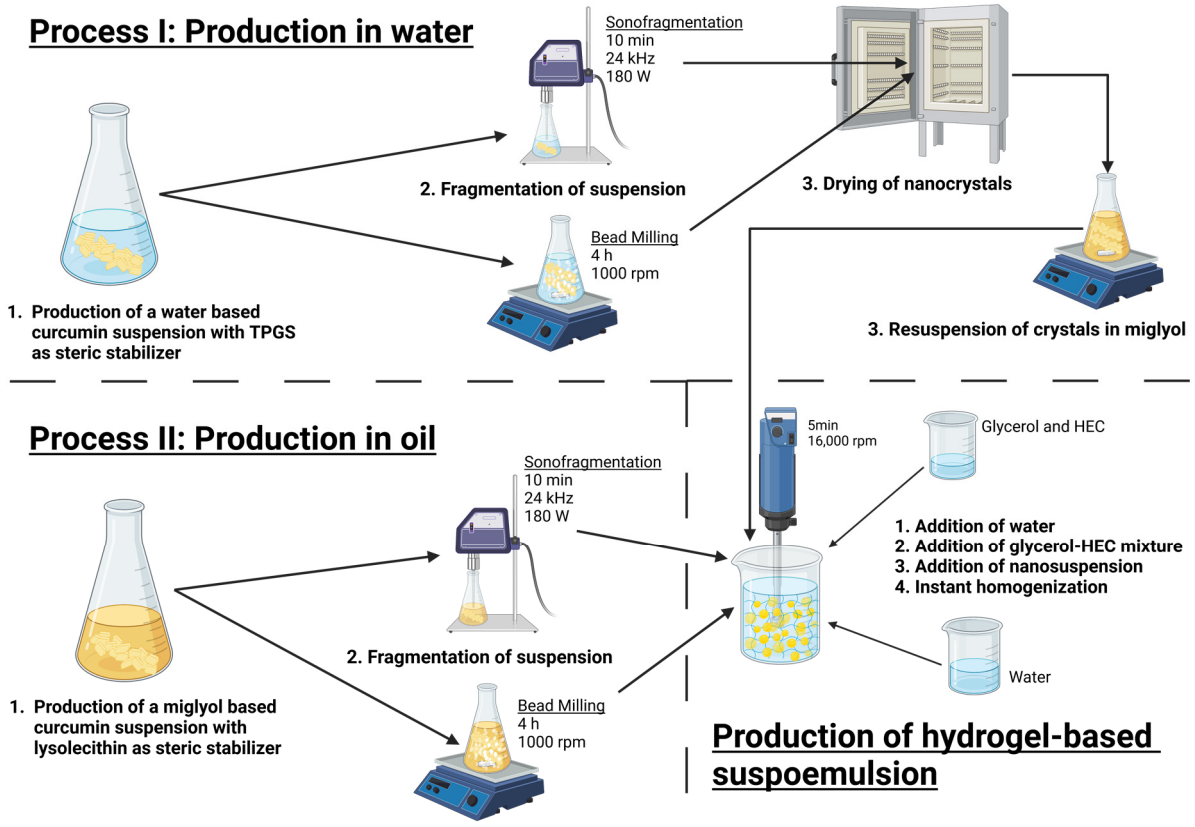

Figure 2. Overview of the different processes. Process I requires additional process steps (drying and resuspension) to transfer the nanocrystals into the oil phase. This is not an element in our study (detailed information in Section 3.1). (The figure was created with BioRender.com).

In the second process, miglyol was used as the continuous phase in which the curcumin was milled. In preliminary tests, we established the most optimal process conditions, including process time, concentration, and intensity, under which the minuscule particles could be produced.

Sonofragmentation

The ultrasonic homogenizer (UP200S, Hielscher Ultrasonics GmbH, Teltow, Germany) used for sonofragmentation was equipped with an S14 horn (max. sound power density: 105 W/cm^2). We used 50 mL of a miglyol-based 10% curcumin suspension. The curcumin–lysolecithin ratio was 1:1 (respectively; in water, TPGS was used). The sonofragmentation device was set at 24 kHz and 180 W at 100% of the adjustable amplitude. The suspension was cooled in an ice bath during fragmentation but the temperature was not further monitored. The process continued for 10 min.

Bead milling

The curcumin nanocrystals were produced using a bead-milling process. The milling was performed with yttrium-stabilized zirconium beads (SiLibeads®; type Zy-P Pharma; 1.0–1.2 mm), which were kindly provided by Sigmund Lindner GmbH (Warmensteinach, Germany), and a magnetic stirring bar (Asteroid 25®; 2 mag AG; München, Germany) in a 100 mL Erlenmeyer flask. Then, 5% bulk curcumin and 5% steric stabilizing agent

(lysolecithin in miglyol and TPGS in water) were added to the flask. Afterward, it was filled up to 100% capacity with miglyol (or, respectively, water). The bead–suspension ratio was 50/50 (*v*/*v*). The mixture was stirred for a total of 4 h at 1000 rpm on a stirring plate (RCT basic; IKA®-Werke; Staufen im Breisgau, Germany); the bead-suspension temperature was kept below 5 °C to avoid reagglomeration effects.

2.2.3. Production of Suspoemulsions

The o/w suspoemulsions were produced based on the formulation shown in Table 1, with dispersed phase fractions of 2% and 10%. The disperse phase always consisted of 5% curcumin, 5% lysolecithin, and 90% miglyol. The continuous phase always consisted of 2.5% HEC, 10% glycerol, and 87.5% water.

Table 1. Formulation of the hydrogel-based o/w suspoemulsion. The SEs were produced with either 10% or 2% dispersal phase.

Phase	Percentage (% (*w*/*w*))	Material	Percentage of Phase (% (*w*/*w*))
Continuous (hydrophile)	90/98	Deionized water	87.5
		Glycerol 85%	10
		HEC (10,000 mPs)	2.5
Disperse (lipophile/suspension)	10/2	Miglyol 812	90
		Curcumin	5
		Lysolecithin	5

The curcumin suspension was stirred for 10 min to achieve a homogeneous phase. The glycerol and hydroxyethylcellulose were weighed together in another beaker and stirred until a homogeneous phase could be observed. The water was added to the glycerol and hydroxyethylcellulose solution (continuous, hydrogel-based phase), followed by the necessary amount of curcumin suspension (dispersed phase). The mixture was instantly homogenized with a T25 digital Ultra-Turrax® rotor-stator homogenizer with the S25N-18G dispersing tool mounted (IKA®- Werke; Staufen im Breisgau, Germany). In this way, we aimed to simultaneously disperse the oil and form a hydrogel in the continuous phase. The complete homogenization process was performed at 16,000 rpm for 5 min.

2.3. Determination of the Encapsulation Efficiency

Establishing a standard curve

A curcumin stock suspension with a concentration of 1 g/L was produced, and 0.005% polysorbate-20 was added. The stock suspension was consecutively diluted to concentrations of 0.5, 0.3, 0.1, 0.05, and 0.01 g/L. The absorption values of those suspensions were then measured in a spectrophotometer (Hελios Gamma; Thermo Spectronic; England, UK) at 500 nm in standard quartz cuvettes. Deionized water was used as a blank.

In preliminary experiments, suspensions of curcumin in water and oil were scanned for their absorbance levels at different wavelengths. At 500 nm, curcumin undergoes absorption in water. On the other hand, absorption in miglyol was nearly zero. Due to this phenomenon, 500 nm was chosen as the wavelength at which to measure.

Determination of encapsulation efficiency

The curcumin concentration in the continuous phase was measured to determine the encapsulation efficiency. The amount of curcumin encapsulated in the oil phase could then be calculated using Equation (1).

$$EE(\%) = \frac{C_{total} - C_{cont.}}{C_{total}} * 100 \quad (1)$$

The encapsulation efficiency (*EE*) was calculated by applying a principle taken from Xu et al. [26]. Differentiating the total curcumin (C_{total}) from the measured amount of curcumin in the continuous phase ($C_{cont.}$), divided by the total amount, gives the encapsulation efficiency (Equation (1)). The dilution factor needed to be incorporated. As a blank, an emulsion without curcumin was used.

The hydrogel-based suspoemulsions were diluted at a ratio of 1:1000 (the SE with 2% (*w/w)* disperse phase was diluted 1:20) with deionized water and stirred on a stirring plate (RCT basic; IKA®–Werke; Staufen im Breisgau, Germany) until a homogenous state was achieved. In the following photometric measuring process (Helios Gamma; Thermo Spectronic; England, UK), an emulsion without curcumin (also diluted in the same ratio) was used as a blank. The diluted SE was measured at 500 nm.

3. Results and Discussion

3.1. Production of the Suspension

Process I: Production in Water

First, curcumin, as received from the manufacturer, was dispersed in water, together with TPGS, using a magnetic stirrer. The suspension was then treated either with ultrasound or with bead milling. The resulting suspensions were directly characterized via laser diffraction analysis. All treatments differed significantly ($p < 0.05$; Kruskal–Wallis test). The bulk crystals had a mean particle size of 16.8 µm ($x_{90.3}$ = 35.3 µm; $x_{10.3}$ = 7.0 µm) and were nearly unimodally distributed (see Figure 3). The bead process created a bimodal distribution of particle sizes; about 78% of the volume consisted of particles of the smaller fraction. Since the ultrasound process had an energy input at least as high as the bead-milling process, and the cavitation of the ultrasound process works well in water, we assumed that the large particles and bimodal particle size distributions resulted from instabilities. Those two fractions could be created by different mechanisms, namely, particle–particle collisions and Ostwald ripening. This is discussed in more detail in the next section. The $x_{50.3}$ was reduced to 0.136 µm with 10% of the total particles measuring smaller than 0.064 µm. The $x_{90.3}$ was reduced to 1.325 µm. The sonofragmentation led to a more unimodal distribution ($x_{10.3}$ = 0.661 µm; $x_{50.3}$ = 8.273 µm; $x_{90.3}$ = 24.772 µm).

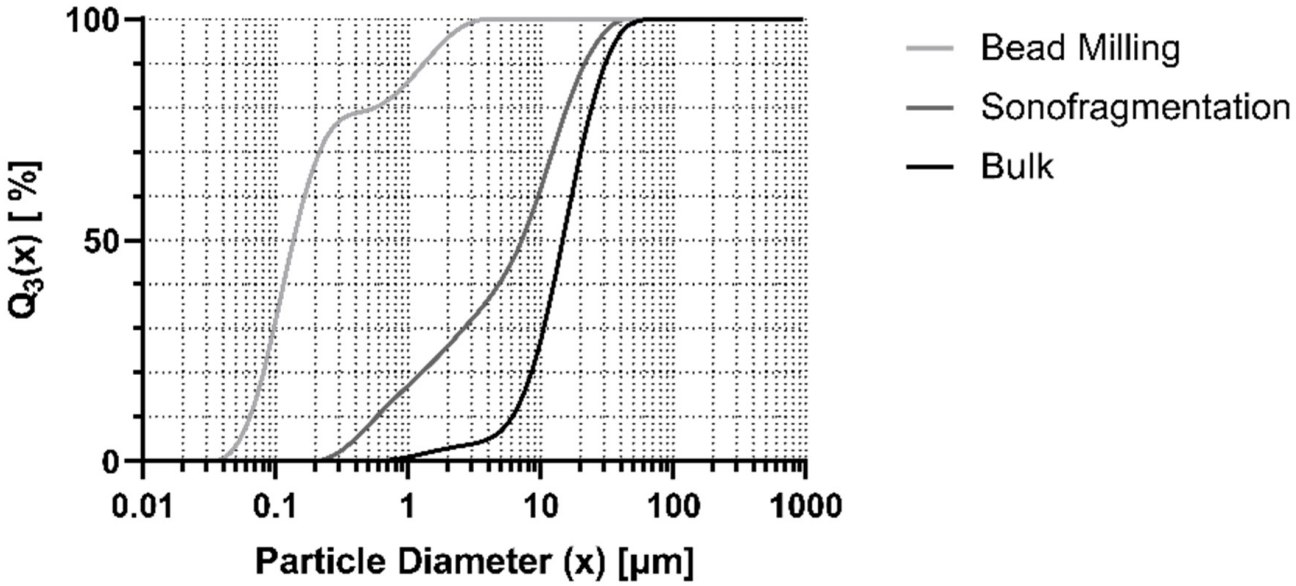

Figure 3. Cumulative particle size distributions of curcumin in water under different treatments, measured using laser diffraction analysis. The relative volume density is plotted against the particle diameter. The black line shows the bulk curcumin, and the dark gray line shows the curcumin after 10 min of sonofragmentation.

Process II: Production in Miglyol

The particle size of the bulk untreated curcumin, the sonofragmented curcumin, and the bead-milled curcumin in oil were measured using laser diffraction analysis. A comparison can be found in Figure 5. Microscopic pictures of the suspensions can be observed in Figure 4. In the untreated curcumin, 80% of particles were larger than 10 µm. The primary particle sizes of the curcumin treated with ultrasonic, bead milling, and bulk curcumin differed significantly ($p < 0.05$; Kruskal–Wallis test).

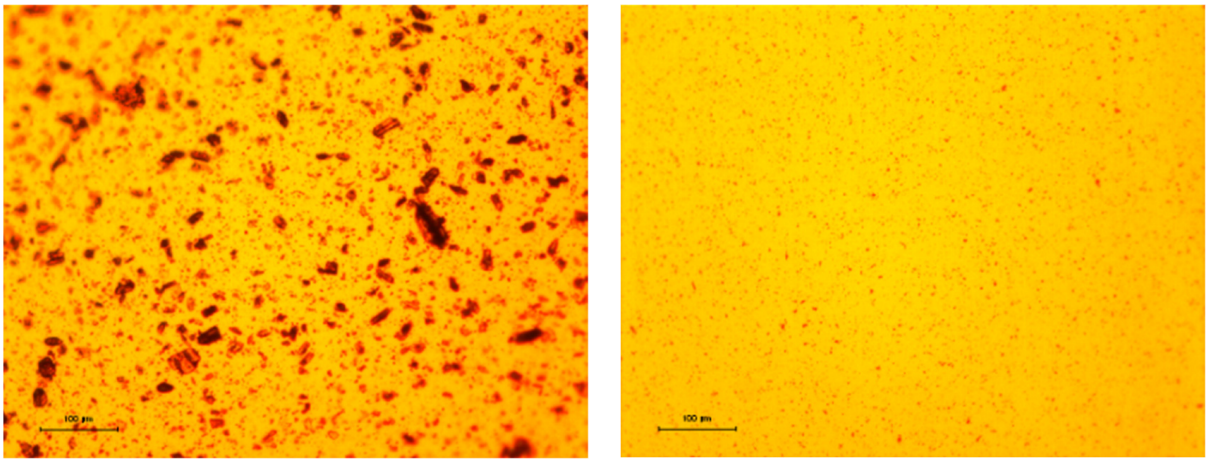

Figure 4. Microscopic picture of the bulk curcumin (**left**) and the bead-milled curcumin (**right**) in miglyol.

The sonofragmentation decreased the $x_{90.3}$ from 35.7 µm (untreated bulk curcumin) to 13.1 µm. The $x_{50.3}$ declined from about 17.5 to 4.2 µm, and the $x_{10.3}$, initially 6.8 µm, decreased to 200 nm. The size distribution was bimodal, with peaks at about 200 nm and 5 µm. The particles in the fraction around 5 µm comprised a larger part of the total volume than the smaller particles belonging to the left population. Initially, we expected smaller particles because of the high-energy input capacity of the ultrasound method. Shin et al. showed smaller particle sizes after ultrasonic treatment [27]. However, the data were not fully comparable because of differences in the dispersant, the type and concentration of stabilizer, power levels, and process times. Additionally, dynamic light scattering (DLS) was used to analyze the sizes, which differed from laser diffraction analysis. However, if we looked only at the fraction around 200 nm, per our measurement, the mean particle size corresponded with data gained by Shin et al. (208 to 246 nm). This comparison could be an indication that the fragmentation was partially successful. A possible explanation for this could be that the lysolecithin absorbed too slowly at the newly gained particle surface. Without a steric stabilizer, the particles could reagglomerate [28].

The bead milling produced higher amounts of nanoparticles, resulting in a left curve shift. The $x_{90.3}$ was 1.4 µm, the $x_{50.3}$ was 76 nm, and the $x_{10.3}$ was 40 nm. The distribution was bimodal, as well. Regarding the total volume, in this case, the smaller particles represented the larger portion of the population. The particle sizes were as expected. In experiments using a similar process, the particles were slightly larger than what we achieved here [15].

The particles must be smaller than the emulsion droplet size in order to achieve a suspoemulsion with the crystals encapsulated in the disperse phase (Figure 1IV). Only about 23% (of the total volume) of the sonofragmented curcumin was smaller than the droplet diameter (Figure 5). In comparison, about 85% of the bead-milled curcumin was smaller (Figure 5). Since we aimed to produce particle sizes lower than the emulsion's droplet diameter ($x_{10.3}$ of 1.4 µm), bead milling is the preferred process.

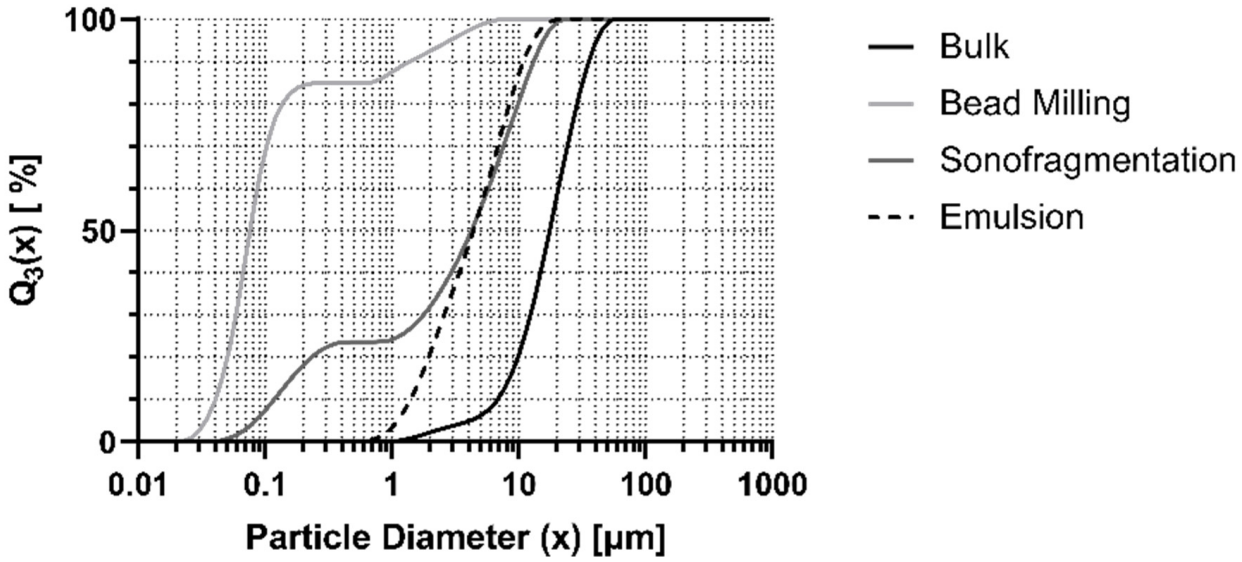

Figure 5. Cumulative particle size distributions of curcumin after different treatments in miglyol, measured using laser diffraction analysis. The relative volume density is plotted against the particle diameter. The black line shows the bulk curcumin, the dark gray line shows the curcumin after 10 min of sonofragmentation, and the light gray line shows the curcumin after 4 h of bead milling. The dashed line indicates the droplet size of the emulsion without curcumin.

A monomodal distribution was desired in order to facilitate a straightforward interpretation of the later encapsulation efficiencies. However, the distributions were bimodal, which could be explained by particle growth processes co-occurring with fragmentation or crystal growth effects based on Ostwald ripening [28].

Particle–particle collisions (especially in bead milling) can explain particle growth [28]. In such cases, strong agglomerates are formed. An equilibrium state can be attained because reagglomeration and fragmentation occur at the same time at specific rates. With increases in milling speed or time, the energy and amount of the growth processes will also increase, resulting in larger particles in the equilibrium state [28].

The aforementioned Ostwald ripening is promoted by an overly high concentration of steric stabilizer [28]. This concentration was present in our study because the lysolecithin functioned as a steric stabilizer as well as an emulsifier at the oil–water interface. This relatively high concentration could not be reduced to stabilize all interfaces (particle–oil and oil–water). This ripening could have resulted in the growth of larger crystals because of the recrystallization of the soluted curcumin. The number of small particles was reduced due to their higher surface area—and, therefore, higher solution pressure—resulting in a higher solubility than that of larger particles.

Nevertheless, this ripening process was unlikely to be observed because the temperature during the milling process was kept constantly under 5 °C. Furthermore, the low temperature decreased curcumin's already low solubility in oil, hampering the Ostwald ripening process [29].

Comparison of Both Processes

Figure 6 directly compares the processes in water (Process I) and oil (Process II). Even when different steric stabilizers (lysolecithin in miglyol and TPGS in water) were used, the particle size distributions of the bulk crystals were roughly the same (as expected) in oil and in water.

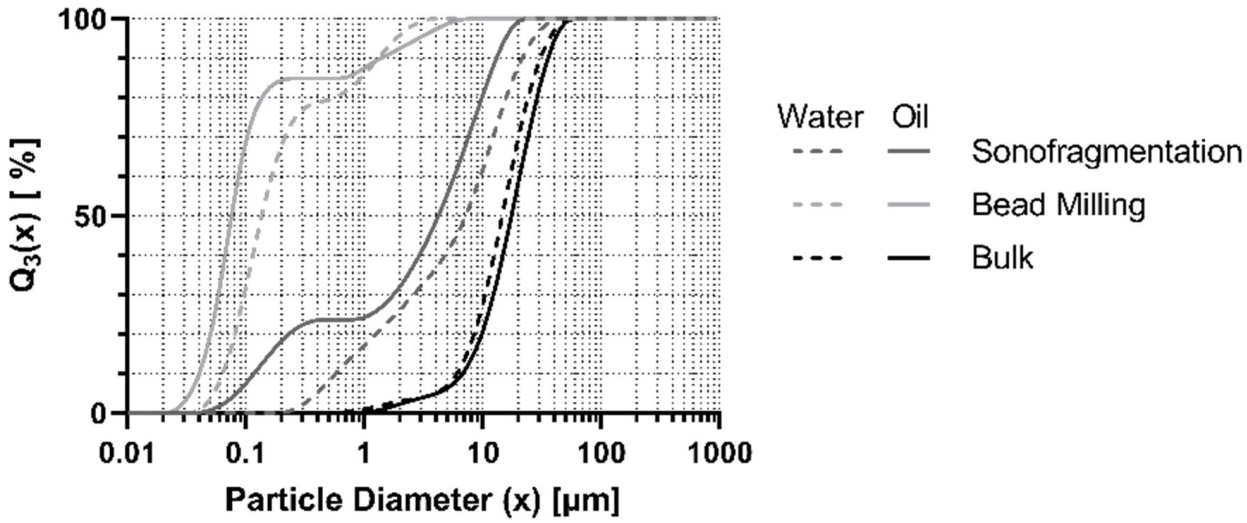

Figure 6. Comparison of the particle size distributions of the two different processes. The relative volume density is plotted against the particle diameter. The dashed lines show Process I, in water, and the filled lines show Process II, in miglyol.

The particle size distribution of the bead-milling-treated crystals in water was shifted to the right in comparison to the distribution in miglyol. Even though the $x_{90.3}$ was higher in miglyol than in water (see previous sections), smaller particles were obtained using the process in miglyol. Additionally, those particles comprised a higher fraction of the total volume of the particles. This could be explained by the higher viscosity of the miglyol, leading to higher shear stresses.

The distributions obtained by sonofragmentation were quite different. Many particles were preserved. In Process II, the treatment in miglyol, we observed a second peak, which was missing when the process was performed in water. The sonofragmentation was expected to be more efficient in water due to the lower vapor pressure, which should have promoted the forming of cavities. However, this was not the case. One possible explanation is that there was a difference in the kinetics of the stabilizers. Lysolectithin could stabilize the newly gained interfaces faster than TPGS. To confirm this, kinetic measurements of the stabilizers at the interfaces would need to be performed. The higher viscosity of miglyol must also be taken into account. The motion of the newly produced nanocrystals was hampered by the higher viscosity, and thus more time was required for them to collide and reagglomerate. The steric stabilizer was not influenced by this effect as much as the particles were, since it was in a soluted state in the miglyol. Therefore, the stabilizer had more time to adsorb on the particle interface.

In any case, when milling in oil, the methods did not only lead to smaller particles, it also had an additional benefit; during production of the actual suspoemulsion, there was no need to transfer the crystals to the oil phase. This could have had a critical influence on the resulting particle size and stability in the final formulation. Therefore, bead milling in miglyol was determined to be the optimal method by which to produce nanocrystals for suspoemulsions.

3.2. Production of Suspoemulsions

As an emulsifier for the o/w emulsion, we chose lysolecithin, which also works as a steric stabilizer on the particles. The use of a second, different emulsifier would have brought with it the risk that displacement effects on the solid–liquid and liquid–liquid interfaces would occur [19]. However, with a hydrophobic–lipophilic balance (HLB) of 6.5–8.0 [30], lysolecithin was classified as a w/o emulsifier rather than an o/w emulsifier. Therefore, the stability of the resulting suspoemulsion was not expected to be sufficiently

high. As a solution, hydroxyethylcellulose was added to the continuous phase as a rheology modifier, producing a high viscosity and a yield point that stabilized the droplets.

The preliminary test also showed stable suspoemulsions with different emulsifiers. Therefore, we attempted to use glycerol monostearate (GMS 60) during the milling process. However, this failed, as the solubility in miglyol was insufficient at the low milling temperatures. Working above the melting point of GMS 60 was not considered a solution. Stability problems were expected due to the rising solubility of curcumin and the possible promotion of Ostwald ripening and other destabilizing effects.

Overall, we were able to produce stable hydrogel-based curcumin-loaded o/w suspoemulsions. Visual inspections of all suspoemulsions produced with lysolecithin (SE with bulk, bead milled, and sonofragmented curcumin) revealed no physical instabilities, such as creaming or sedimentation, after four weeks. All SE were homogenous and could not be distinguished with the unaided eye (Figure A1).

3.3. Determination of the Encapsulation Efficiency

In the first method, we took advantage of the fact that curcumin has a different optical absorption in water than in oil. Therefore, only the curcumin in water could be detected if we measured at a wavelength of 500 nm. This effect could allow us to determine the amount of lost curcumin in the water.

The preparation of the dilution series was carried out three times. A pooled linear regression was performed using the measured absorptions (Y = 0.8640X + 0.008708), as shown in Figure A2. The degree of determination (R2) was 0.9952, with a standard error for the slope of 0.01670. The standard error for the Y-interception was 0.004435. The deviation from zero was significant ($p < 0.0001$). The dilution of the produced suspoemulsions was performed in high ratios. This high dilution had to be used because of the turbidity of the emulsion, which was, in turn, due to its droplets. In the 10% suspoemulsion, the dilution rate utilized was 1:1000, in an attempt to obtain a sufficiently significant transmission signal to permit measurement. However, due to the high dilution, the absorption of the curcumin was not high enough to achieve sufficient measurement sensitivity. It was constantly beneath the calibration line. The calibration line could not be extended for lower concentrations because of its limited accuracy. Hence, suspoemulsions with only 2% (*w/w*) dispersal phase were produced to avoid this issue. The dilution rate could be reduced to 1:20. However, the absorption rates of the samples were not constant and had an extensive range. Even negative absorptions were measured (Table A1). The well-known reason for this problem is that Lambert–Beer's Law is only valid for samples without (or with negligible) scattering [31]. In conclusion, the method did not produce any scientifically significant results.

For a solution, we attempted to separate the oil from the water with centrifugation, but the separation resulted in a transfer of curcumin between the phases. Therefore, the original encapsulation efficiency could not be measured. Until a method is found to separate oil from water without transferring curcumin between phases, photometric measurement is not convenient for this purpose.

A second approach was to measure the encapsulation efficiency using rheology. In principle, it is known that particles influence the rheology of gels and emulsions [32]. Therefore, the idea was to determine to what extent differences in rheological behavior could provide information about the location of particles in gel or oil droplets. For this purpose, oscillatory and rotational rheometric measurements were carried out. However, with the rheological equipment available, no significant differences were found between individual samples.

We propose that NMR spectroscopy (nuclear magnetic resonance) or Raman microscopy could be appropriate methods to evaluate the encapsulation efficiency in suspoemulsions. Therefore, further research is needed to elucidate this in more detail.

4. Conclusions

This study investigated curcumin suspension production in both oil and water to produce stable hydrogel-based curcumin-loaded o/w suspoemulsions. We were able to show that the production process in oil led to smaller particles than using water. This can be explained by the fact that stabilization in the oil was better due to the oil's higher viscosity. Furthermore, the bead-milling process, at the chosen parameters, led to smaller particles than sonofragmentation. Directly producing an oil-based suspension was the more straightforward means of production, as opposed to drying and then redispersing curcumin into the oil, as associated problems could thus be avoided. The achieved bimodal distribution was not optimal for particle size stability because of its susceptibility to Ostwald ripening. Further studies could investigate whether or not a combination of bead milling and sonofragmentation could lead to narrower particle size distributions or a monomodal distribution.

Suspoemulsions with different curcumin particle sizes were produced. All the suspoemulsions were physically stable and could not be macroscopically distinguished. However, the encapsulation efficiency could not be determined with photometric measurements or rheology methods. For this, an alternative method must be developed in future studies. Therefore, we propose, as a future undertaking, NMR spectroscopy or Raman spectroscopy as appropriate methods. In addition, as a follow-up study, dermal penetration studies with ex vivo models could be used to show the possible benefits of this system against classical nanosuspensions.

Author Contributions: Conceptualization, K.K. and C.M.K.; methodology, T.B. and S.F.H.; formal analysis, all authors; investigation, T.B. and C.M.K.; resources, T.B. and K.K.; writing—original draft preparation, T.B. and K.K.; writing—review and editing, C.M.K., S.F.H. and M.K.; visualization, T.B. and K.K.; supervision, K.K. All authors have read and agreed to the published version of the manuscript.

Funding: This research received no external funding.

Acknowledgments: The authors wish to extend their thanks to C. Meier, M. Scherer, and N. Ströhle for the preliminary tests.

Conflicts of Interest: The authors declare no conflict of interest.

Appendix A

Figure A1. A hydrogel-based suspoemulsion with bead-milled curcumin four weeks after its production. The suspoemulsions with sonofragmented or bulk curcumin do not differ macroscopically from the picture shown.

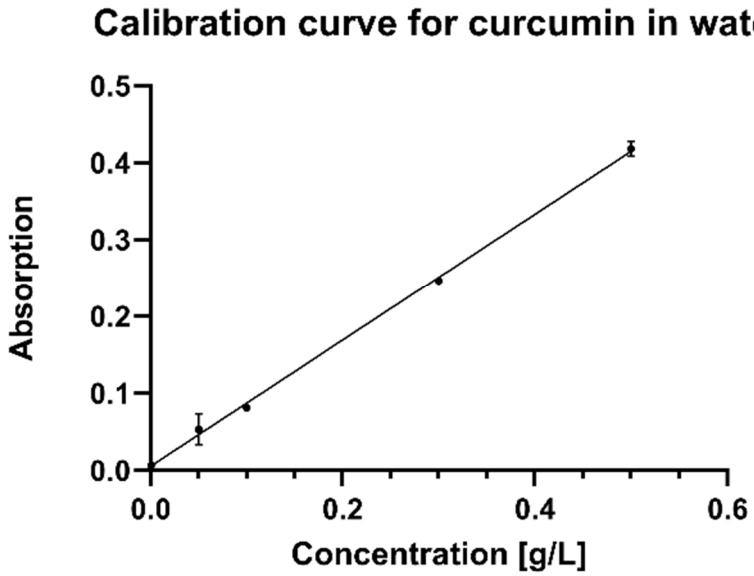

Figure A2. Absorption, plotted against the curcumin concentration in water. The measurement is performed using a UV-VIS spectrometer at 500 nm. The fitted linear regression has a degree of determination of 0.9952.

Table A1. Results of the photometric measurement of the EE of a 2% SE with bulk curcumin. The $c_{cont.}$ is already corrected with the dilution factor.

n	$A_{500\ nm}$	Real Dilution Factor	c_{total} (g/kg$_{SE}$)	$c_{cont.}$ (Measured) (g/kg$_{SE}$)	EE (%)
1	0.032	20.03	1.007	0.943	−1775.67
2	−0.109	19.99	1.002	−2.938	393.17
3	−0.046	19.94	0.999	27.554	−2656.44
4	−0.049	20.45	1.001	−1.316	231.50
5	0.022	19.70	1.002	0.657	34.48

References

1. Müller, R.; Keck, C. Twenty years of drug nanocrystals: Where are we, and where do we go? *Eur. J. Pharm. Biopharm.* **2012**, *80*, 1–3. [CrossRef] [PubMed]
2. Wahlang, B.; Pawar, Y.B.; Bansal, A.K. Identification of permeability-related hurdles in oral delivery of curcumin using the Caco-2 cell model. *Eur. J. Pharm. Biopharm.* **2010**, *77*, 275–282. [CrossRef] [PubMed]
3. Ahmed, T.; Gilani, A. Therapeutic Potential of Turmeric in Alzheimer's Disease: Curcumin or Curcuminoids? *Phytother. Res.* **2014**, *28*, 517–525. [CrossRef] [PubMed]
4. Plummer, S.M.; Holloway, K.A.; Manson, M.M.; Munks, R.J.; Kaptein, A.; Farrow, S.; Howells, L. Inhibition of cyclo-oxygenase 2 expression in colon cells by the chemopreventive agent curcumin involves inhibition of NF-κB activation via the NIK/IKK signalling complex. *Oncogene* **1999**, *18*, 6013–6020. [CrossRef] [PubMed]
5. Sahebkar, A.; Serban, M.-C.; Ursoniu, S.; Banach, M. Effect of curcuminoids on oxidative stress: A systematic review and meta-analysis of randomized controlled trials. *J. Funct. Foods* **2015**, *18*, 898–909. [CrossRef]
6. Shehzad, A.; Lee, J.; Lee, Y.S. Curcumin in various cancers. *Biofactors* **2013**, *39*, 56–68. [CrossRef]
7. *EMA/HMPC/749518/2016*; Assessment Report on *Curcuma longa* L., Rhizoma. European Medicines Agency (EMA): Zuidas, Amsterdam, 25 September 2018.
8. Shome, S.; Das Talukdar, A.; Choudhury, M.D.; Bhattacharya, M.K.; Upadhyaya, H. Curcumin as potential therapeutic natural product: A nanobiotechnological perspective. *J. Pharm. Pharmacol.* **2016**, *68*, 1481–1500. [CrossRef]
9. Sadigh, M.K.; Zakerhamidi, M.; Shamkhali, A.; Babaei, E. Photo-physical behaviors of various active forms of curcumin in polar and low polar environments. *J. Photochem. Photobiol. A: Chem.* **2017**, *348*, 188–198. [CrossRef]
10. Nayak, A.; Mills, T.; Norton, I. Lipid Based Nanosystems for Curcumin: Past, Present and Future. *Curr. Pharm. Des.* **2016**, *22*, 4247–4256. [CrossRef]
11. Anand, P.; Nair, H.B.; Sung, B.; Kunnumakkara, A.B.; Yadav, V.R.; Tekmal, R.R.; Aggarwal, B.B. RETRACTED: Design of curcumin-loaded PLGA nanoparticles formulation with enhanced cellular uptake, and increased bioactivity in vitro and superior bioavailability in vivo. *Biochem. Pharmacol.* **2010**, *79*, 330–338. [CrossRef]

12. Araiza-Calahorra, A.; Akhtar, M.; Sarkar, A. Recent advances in emulsion-based delivery approaches for curcumin: From encapsulation to bioaccessibility. *Trends Food Sci. Technol.* **2018**, *71*, 155–169. [CrossRef]
13. Im, K.; Ravi, A.; Kumar, D.; Kuttan, R.; Maliakel, B. An enhanced bioavailable formulation of curcumin using fenugreek-derived soluble dietary fibre. *J. Funct. Foods* **2012**, *4*, 348–357. [CrossRef]
14. Eckert, R.W.; Wiemann, S.; Keck, C.M. Improved Dermal and Transdermal Delivery of Curcumin with SmartFilms and Nanocrystals. *Molecules* **2021**, *26*, 1633. [CrossRef] [PubMed]
15. Pelikh, O.; Keck, C.M. Hair Follicle Targeting and Dermal Drug Delivery with Curcumin Drug Nanocrystals—Essential Influence of Excipients. *Nanomaterials* **2020**, *10*, 2323. [CrossRef] [PubMed]
16. Vidlářová, L.; Romero, G.B.; Hanuš, J.; Štěpánek, F.; Müller, R.H. Nanocrystals for dermal penetration enhancement–Effect of concentration and underlying mechanisms using curcumin as model. *Eur. J. Pharm. Biopharm.* **2016**, *104*, 216–225. [CrossRef]
17. Bratz, M.; Parg, A.; Fricke, M. Suspoemulsions: Key Technology for Tailor-Made Ready-Mix Formulations. In *Chemistry of Crop protection: Progress and Prospects in Science and Regulation*; Voss, G., Ramos, G., Eds.; Documents Thirty Invited Lectures Held at the 10th IUPAC International Congress on the Chemistry of Crop Protection in August 2002; Wiley: Hoboken, NJ, USA, 2003; pp. 262–271. [CrossRef]
18. A Faers, M.; Pontzen, R. Factors influencing the association between active ingredient and adjuvant in the leaf deposit of adjuvant-containing suspoemulsion formulations. *Pest Manag. Sci.* **2008**, *64*, 820–833. [CrossRef]
19. Tadros, T.F. Formulation Science and Technology. 6. Formulation of Suspoemulsions. In *Volume 4: Agrochemicals, Paints and Coatings and Food Colloids*; De Gruyter: Berlin, Germany; Boston, MA, USA, 2018. [CrossRef]
20. Schmidt, P.C.; Perschbacher, H.; Steffens, K.J.; Kraemer, H.P. Developement of a Suspension-Emulsion System for Parental Application in Animals. *Acta Pharm. Technol.* **1989**, *35*, 34–37.
21. Turino, L.N.; Mariano, R.N.; Mengatto, L.N.; Luna, J.A. *In vitro* evaluation of suspoemulsions for *in situ*-forming polymeric microspheres and controlled release of progesterone. *J. Microencapsul.* **2015**, *32*, 538–546. [CrossRef]
22. Intarakumhaeng, R.; Shi, Z.; Wanasathop, A.; Stella, Q.; Wei, K.S.; Styczynski, P.B.; Li, C.; Smith, E.D.; Li, S. In vitro skin penetration of petrolatum and soybean oil and effects of glyceryl monooleate. *Int. J. Cosmet. Sci.* **2018**, *40*, 367–376. [CrossRef]
23. Patzelt, A.; Lademann, J.; Richter, H.; Darvin, M.E.; Schanzer, S.; Thiede, G.; Sterry, W.; Vergou, T.; Hauser, M. In vivo investigations on the penetration of various oils and their influence on the skin barrier. *Ski. Res. Technol.* **2012**, *18*, 364–369. [CrossRef]
24. Lopes, L.; Murphy, N.; Nornoo, A. Enhancement of transdermal delivery of progesterone using medium-chain mono and diglycerides as skin penetration enhancers. *Pharm. Dev. Technol.* **2009**, *14*, 524–529. [CrossRef]
25. Schilde, C.; Mages-Sauter, C.; Kwade, A.; Schuchmann, H. Efficiency of different dispersing devices for dispersing nanosized silica and alumina. *Powder Technol.* **2011**, *207*, 353–361. [CrossRef]
26. Xu, W.; Huang, L.; Jin, W.; Ge, P.; Shah, B.R.; Zhu, D.; Jing, J. Encapsulation and release behavior of curcumin based on nanoemulsions-filled alginate hydrogel beads. *Int. J. Biol. Macromol.* **2019**, *134*, 210–215. [CrossRef] [PubMed]
27. Shin, G.H.; Li, J.; Cho, J.H.; Kim, J.T.; Park, H.J. Enhancement of Curcumin Solubility by Phase Change from Crystalline to Amorphous in Cur-TPGS Nanosuspension. *J. Food Sci.* **2016**, *81*, N494–N501. [CrossRef] [PubMed]
28. Peltonen, L.; Hirvonen, J.T. Pharmaceutical nanocrystals by nanomilling: Critical process parameters, particle fracturing and stabilization methods. *J. Pharm. Pharmacol.* **2010**, *62*, 1569–1579. [CrossRef] [PubMed]
29. Taylor, P. Ostwald ripening in emulsions: Estimation of solution thermodynamics of the disperse phase. *Adv. Colloid Interface Sci.* **2003**, *106*, 261–285. [CrossRef] [PubMed]
30. Jala, R.C.R.; Chen, B.; Li, H.; Zhang, Y.; Cheong, L.-Z.; Yang, T.; Xu, X. Enzymatic preparation and characterization of soybean lecithin-based emulsifiers. *Grasas Aceites* **2016**, *67*, 168. [CrossRef]
31. Mäntele, W.; Deniz, E. UV–VIS absorption spectroscopy: Lambert-Beer reloaded. *Spectrochim. Acta Part A Mol. Biomol. Spectrosc.* **2017**, *173*, 965–968. [CrossRef]
32. Münstedt, H. Rheological Measurements and Structural Analysis of Polymeric Materials. *Polymers* **2021**, *13*, 1123. [CrossRef]